7. SUMMARY AND CONCLUSION

The stethoscope remains the centerpiece of diagnostic tools for clinicians performing cardiac examinations of their patients. Many cardiac and pulmonary abnormalities can be diagnosed at the bedside with the use of the stethoscope. Auscultation is one of the most cost-effective diagnostic tests for patients with cardiac and pulmonary abnormalities.

Digital stethoscopes are designed to overcome the disadvantages of the acoustic stethoscopes. Digital stethoscope electronically amplifies body sounds. Digital stethoscope uses sound waves, which are converted from analog to electrical signals that are amplified and provide much lauder and clearer sound. This makes identifying problems quicker and easier, and it allows the recording and playback of sounds picked up, making it useful for references or in the teaching for students.

In the present work, digital stethoscope system was designed and constructed. It consists of a function generator circuit for generating a sound signal with appropriate frequency and waveform to the constructed lung model by a mini-speaker inserted into the simulated trachea. Electrets condenser microphone at the surface of the model receives the sound signal and converts it into an electric signal. The signal then was amplified and filtered with a suitable gain and transmitted through an electrical cable to the sound card of a personal computer for further monitoring and analysis of the output sound signal.

The results of the simulated model showed that:

- The amplitude of the output sound signal increases with the increasing of solutions (Water, Sodium chloride, Glucose), and gel quantity.
- The sound attenuation decreases with the increasing of solutions quantity.
- The coefficient of attenuation decreases with the increasing of solutions quantity.

Digital stethoscope array system was developed for monitoring and diagnosing obstructive lung diseases which are associated with accumulation of lung fluids and cardiovascular diseases which associated with heart murmur like systolic and diastolic murmur from different auscultation points. Parameters such as sound attenuation and attenuation coefficient

The results of heart sound analysis showed that:

- The frequency spectrums of all normal and abnormal heart sounds were 64 Hz.
- The amplitude of normal heart sound at the apex auscultation point was -17 dB, while at the aortic and pulmonic auscultation points were -10 dB.
- The amplitude of abnormal heart sounds S3 and S4 at the apex auscultation point were -18dB.
- The amplitude of split S1 at the apex auscultation point was -22 dB, while the amplitude of split S2 at the pulmonic auscultation point was -16 dB.

- The amplitude of early, mid, late and holo systolic murmur at the apex auscultation point were in the range of -24 dB to -22 dB.

The results of lung sound analysis showed that:

- The amplitude of all normal and abnormal lung sounds was in the range of -50 dB to -30 dB.
- The frequency spectrum of normal vesicular lung sound was 120 Hz.
- The frequency spectrum of coarse crackles sound was 330 Hz.
- The frequency spectrum of inspiratory stridor sound was 275 Hz.
- The frequency spectrum of pleural friction sound was 58 Hz.
- The frequency spectrum of wheezing sound was 198 Hz.

8. REFERENCES

1. Bergstresser T, Ofengeim D, Vyshedskiy A, Shane J, Murphy R. Sound Transmission in the Lung as a Function of Lung Volume. J Appl Physiol. 2002;93(2) 667-74.

2. Martinez-Alajarin J, Lopez-Candel J, Ruiz-Merino R. Classification and Diagnosis of Heart Sounds and Murmurs Using Artificial Neural Networks. Springer Link 2007, pp. 303-12.

3. Leuppi J, Dieterle T, Wildeisen I, et al. Can Airway Obstruction be Estimated by Lung Auscultation in an Emergency Room Setting? Respir Med. 2005; 100(2) 279-85.

4. Bray D, Reilly RB, Haskin L, McCormack B. Assessing Motility Through Abdominal Sound Monitoring. IEEE EMBS 1997; (6)2398-400.

5. L.A. Geddes. "Birth of stethoscope." IEEE Engineering in Medicine and Biology Magazine. 2005, 24(1), 84‑86.

6. Jay V. The legacy of Laënnec. Arch Pathol Lab Med 2000;124:1420-1421.

7. Bloch H. The inventor of the stethoscope: Rene Laënnec. J Fam Pract 1993;37:191.

8. Welsby PD, Parry G, Smith D. The stethoscope: some preliminary investigations. Postgrad Med J 2003;79:695-698.

9. Dalmay F, Antonini MT, Marquet P. Acoustic properties of the normal chest. Eur Respir J 1995; 8, 1761–1769.

10. Sterne J. Mediate Auscultation, the Stethoscope, and the "Autopsy of the Living": Medicine's Acoustic Culture. Journal of Medical Humanities 2012; 2(22). 115 – 136

11. Westhorpe R, Ball C. Precordial and Oesophageal Stethoscopes. Anaethesia and Intensive Care, 2008; 4(36), 479 – 486.

12. Rappaport M, Sprague H. Physiologic and physical laws that govern auscultation, and their clinical application. The acoustic stethoscope and the electrical amplifying stethoscope and stethograph. American Heart Journal, 1941; 3(21), 257-318.

13. Bishop P. Evolution of the stethoscope. Journal of the Royal Society of Medicine. 1980; 73, pp 448.

14. Frederick H, Dodge H. "The stethophone," an electrical stethoscope. Bell Sys Tech J 1924; 3: 531.

15- Johnston, F, Kline, E. An acoustical study of the stethoscope. Arch Intern Med 1940; 65: 328.

16. Rappaport M, Sprague H. Physiologic and physical laws that govern auscultation, and their application. Amer Heart J 1941; 21: 257.

17. Rappaport M, Sprague H. The effects of tubing bore on stethoscope efficiency. Amer Heart J 1951; 42: 605.

18. Groom D. What constitutes an efficient stethoscope? In The Theory and Practice of Auscultation, edited by B. L. Segal. Philadelphia, F. A. Davis Co., 1964; p. 291.

19. Groom D. Effect of background noise on cardiac auscultation. Amer Heart J 1956; 52: 781.

20. Bishop. Evolution of the Stethoscope. Journal of the Royal Society of Medicine. 1980; 73:448-456.

21. Druzgalski C, Donnerberg R, Campbell R. Techniques of recording respiratory sounds. J Clin Eng 1980; 5: 321–333.

22. Leblanc P, Macklem P, Ross W. Breath sounds and distribution of pulmonary ventilation. Am Rev Respir Dis 1970; 102: 10–16.

23. Cugell D. Use of tape-recordings of respiratory sound and breathing pattern for instruction in pulmonary auscultation. Am Rev Respir Dis 1971; 104: 948–950.

24. McKusick V, Jenkins J, Webb G. The acoustic basis of the chest examination: studies by means of sound spectrography. Am Rev Tuberc 1955; 72: 12–34.

25. Abella M, Formolo J, Penney D. Comparison of the acoustic properties of six popular stethoscopes. J Acoust Soc Am 1992; 91(4 Pt 1):2224-2228.

26. Welsby P, Parry G, Smith D. The stethoscope: some preliminary investigations. Postgrad Med J 2003; 79(938):695-698.

27. Hong C, Wang W, Zhong N. the invention and evolution of the stethoscope. Pub med 2010; 40(6):337-340.

28. Jatupaiboon N., Pan-ngum S., Israsena P. Electronic stethoscope prototype with adaptive noise cancellation. 8th International Conference on ICT and Knowledge Engineering, 2010; pp: 32 – 36.

29. Shier D, Butler J, Lewis R. Human anatomy & physiology, 11th ed. 2007: p 764.

30. Tu J, Inthafong K, Ahmadi G. Computational fluid and particle dynamics in the human respiratory system, 2013: p 251.

31. Bergstresser T, Ofengeim D, Vyshedskiy A. Sound transmission in the lung as a function of lung volume, J. Appl. Physiol. 2002; 93, 667-674.

32. Gavriely N, Nissan M, Rubin A. Spectral characteristics of chest wall breath sounds in normal subjects. Thorax 1995; 50:1292-300.

33. Austrheim O, Kraman S. The effect of low density gas breathing on vesicular lung sounds. Respir Physiol 1985; 60:145-55.

34. Bohadana A, Kanga J, Kraman S. Does airway closure affect lung sound generation? Clin Physiol 1988; 8:341-9.

35. Pasterkamp H, Sanchez I. Effect of gas density on respiratory sounds. Am J Respir Crit Care Med 1996; 153:1087-92.

36. Bohadana A, Peslin R, Uffholtz H. Breath sounds in the clinical assessment of airflow obstruction. Thorax 1978; 33: 345-51.

37. V.P. Harper, H. Pasterkamp, H. Kiyokawa, and G.R. Wodicka, "Modeling and measurement of flow effects on tracheal sounds," IEEE Journal of Biomedical Engineering, 2003; 50: 1-10.

38. Beck R, Rosenhouse G, Mahagnah M. "Measurements and theory of normal tracheal breath sounds," Ann Biomed Eng, 2005; 33: 1344-1351.

39. Yadollahi A. "A robust method for estimating respiratory flow using tracheal sound entropy," IEEE Transactions on Biomedical Engineering, 2006; 53: 662-668.

40. Kandaswamy A, Kumar C, Ramanathan R. Neural classification of lung sounds using wavelet coefficients. Comput Biol Med 2004; 34: 523- 537.

41. Taplidou S, Hadjileontiadis L. Wheeze detection based on time-frequency analysis of breath sounds. Comput Biol Med 2007; 37: 1073-1083.

42. Taplidou S, Hadjileontiadis L. Nonlinear analysis of wheezes using wavelet bicoherence. Comput Biol Med 2007; 37: 563-570.

43. Charbonneau G, Ademovic E, Cheetham B. Basic techniques for respiratory sound analysis. Eur Respir Rev, 2000; 10: 625- 635.

44. Oud M, Doijes E. Automated breath sound analysis. Proceedings of 18th Annual International Conference of IEEE Engineering in Medicine and Biology Society. Amsterdam, 1996; 990-992.

45. Sovijärvi A, Dalmasso F, Vanderschoot J. Definition of terms for application of respiratory sounds. Eur Respir Rev 2000; 10: 597-610.

46. Pasterkamp H, Kraman S, Wodicka G. Respiratory sounds. Advances beyond the stethoscope. Am J Respir Crit Care Med 1997; 156: 974-987.

47. Baughman R, Loudon R. Stridor: differentiation from asthma or upper airway noise. Am Rev Respir Dis 1989; 139: 1407-9.

48. Morris M, Christopher K. Diagnostic criteria for the classification of vocal cord dysfunction. Chest 2010; 138: 1213-23.

49. Butani L, O'Connell E. Functional respiratory disorders. Ann Allergy Asthma Immunol 1997; 79:91-9.

50. Forgacs P. The functional basis of pulmonary sounds. Chest 1978; 73:399-405.

51. Gavriely N, Shee T, Cugell D. Flutter in flow-limited collapsible tubes: a mechanism for generation of wheezes. J Appl Physiol 1989; 66:2251-61.

52. Ravenna F, Caramori G, Panella G, et al. An unusual case of congenital short trachea with very long bronchi mimicking bronchial asthma. Thorax 2002; 57:372-3.

53. Munakata M, Ukita H, Doi I, et al. Spectral and waveform characteristics of fine and coarse crackles. Thorax 1991; 46: 651-7.

54. Vyshedskiy A, Alhashem R, Paciej R, et al. Mechanism of inspiratory and expiratory crackles. Chest 2009; 135:156- 64.

55. Cottin V, Cordier J. Velcro crackles: the key for early diagnosis of idiopathic pulmonary fibrosis? Eur Respir J 2012; 40: 519-21.

56. Flietstra B, Markuzon N, Vyshedskiy A. Automated analysis of crackles in patients with interstitial pulmonary fibrosis. Pulm Med 2011; 590-606.

57. Epler G, McLoud T, Gaensler E. Normal chest roentgenograms in chronic diffuse infiltrative lung disease. N Engl J Med 1978; 298:934-9.

58. Al Jarad N, Strickland B, Bothamley G. Diagnosis of asbestosis by a time expanded wave form analysis, auscultation and high resolution computed tomography: a comparative study. Thorax 1993; 48:347-53.

59. Murphy R, Gaensler E, Holford S. Crackles in the early detection of asbestosis. Am Rev Respir Dis 1984; 129:375-9.

60. Piirilä P. Changes in crackle characteristics during the clinical course of pneumonia. Chest 1992; 102:176-83.

61. Murphy R, Vyshedskiy A. Acoustic findings in a patient with radiation pneumonitis. N Engl J Med 2010; 363(20):e31.

62. Earis J, Marsh K, Pearson M. The inspiratory "squawk" in extrinsic allergic alveolitis and other pulmonary fibroses. Thorax 1982; 37: 923-6.

63. Paciej R, Vyshedskiy A, Bana D. Squawks in pneumonia. Thorax 2004; 59: 177-8.

64. Edwards W. Anatomy of the Cardiovascular System; Clinical Medicine, Harper & Row, Philadelphia, 1984; 6: 1–24.

65. Malouf J, Edwards W, Tajil A. Functional anatomy of the heart. In Fuster , Alexander R, O'Rourke R (eds), Hurst's: The Heart, 10th edn. McGraw- Hill Inc. 2001; pp. 19–62.

66. Boulpaep E. Organisation of 4. Cardiovascular System. Boron WF, Boulpaep EL, updated version. Elsevier Saunders, 2005; pp. 423–507.

67. Tortora G, Grabowski S. Principles of Anatomy and Physiology, 8th edn. HarperCollins College Publishers, New York, 1996; pp. 598–600.

68. Bullock J, Boyle J, Wang M. Physiology, The National Medical Series for Independent Study, 2nd edn. Williams and Wilkins, 1991; pp. 93–148.

69. Edwards WD. Anatomy of the Cardiovascular System; Clinical Medicine, Harper & Row, Philadelphia, 1984; 6: 1–24.

70. Boulpaep E. Organisation of 4. Cardiovascular System. Boron WF, Boulpaep EL, updated version. Elsevier Saunders, 2005; pp. 423–507.

71. Edwards W. Cardiac anatomy and examination of cardiac specimens. In Emmanouilides G et al. (eds). Moss & Adams Heart Diseae in Infants, Children and Adolescents, 5th edn. Williams & Wilkins, Baltimore, 1995; pp. 70–105.

72. Malouf J, Edwards W, Tajil A. Functional anatomy of the heart. In Fuster F, Alexander RW, O'Rourke RA (eds), Hurst's: The Heart, 10th edn. McGraw- Hill Inc., 2001; pp. 19–62.

73. Bullock J, Boyle J , Wang M. Physiology, The National Medical Series for Independent Study, 2nd edn. Williams and Wilkins, 1991; pp. 93–148.

74. Gray's P. In Gray's Anatomy, 38th edn. Churchill Livingston, New York, 1995; pp.1498.

75. Widmaier E, Raff H, Strang K. Cardiovascular physiology. In Vanders Human Physiology – The Mechanism of Body Function, 10th edn. McGraw-Hill, 2006; pp. 387–476.

76. Apkon M. Cellular physiology of skeletal, cardiac and smooth muscle. In Boron WF, Boulpaep EL (eds), Medical Physiology. Elsevier Saunders, 2005; pp. 230–254.

77. Edwards W. Anatomic basis for tomographic analysis of the heart at autopsy. Cardiol Clin, 1984; 2:485–506.

78. Sharif Z, Zainal M, Sha'ameri A. Analysis and classification of heart sounds and murmurs based on the instantaneous energy and frequency estimations, Proc. of IEEE TENCON, 2000; 2: 130-134.

79. Ahlstrom C, Hult P, Rask P. Feature extraction for systolic heart murmur classification, Annals of Biomedical Engineering, 2006; 34: 1666 -1677.

80. Comak E, Arslan A. A decision support system based on support machines for diagnosis of the heart valve diseases, Computers in Biology and Medicine, 2007; 37: 21-27.

81. Sinha R, Aggarwal Y, Das B. Back propagation artificial neural network classi_er to detect changes in heart sound due to mitral valve regurgitation, Journal of Medical Systems, 2007; 31:205-209.

82. Schreur H, Sterk P, Vanderschoot J, et al. Lung sound intensity in patients with emphysema and in normal subjects at standardised airflows. Thorax 1992; 47:674–9.

83. Barnes, P. Chronic obstructive pulmonary disease: a growing but neglected epidemic. PLoS Med, 2007; 4: e112.

84. Mannino, D, Buist, A. Global burden of COPD: risk factors, prevalence, and future trends. Lancet, 2007; 370: 765–773.

85. Pearce N. Worldwide trends in the prevalence of asthma symptoms: phase III of the International Study of Asthma and Allergies in Childhood (ISAAC). Thorax, 2007; 62: 758–766.

86. Kraft M. Asthma and chronic obstructive pulmonary disease exhibit common origins in any country! Am. J. Respir. Crit. Care Med, 2006; 174: 238–240.

87. Barnes P. Against the Dutch hypothesis: asthma and chronic obstructive pulmonary disease are distinct diseases. Am. J. Respir. Crit. Care. Med, 2006; 174: 240–243.

88. Barnes P. Mechanisms in COPD: differences from asthma. Chest, 2000; 117: 10–14.

89. Jeffery P. Comparison of the structural and inflammatory features of COPD and asthma. Chest, 2000; 117: 251–260.

90. Wenzel S. Asthma: defining of the persistent adult phenotypes. Lancet, 2006; 368: 804–813.

91. Phelan P, Robertson C, Olinsky A. The Melbourne Asthma Study: 1964–1999. J. Allergy Clin. Immunol. 2002; 109: 189–194.

92. Pearson SB, Pearson EM, Mitchell JR. The diagnosis and management of patients admitted to the hospital with acute breathlessness. Postgrad Med J 1981; 57:419–24.

93. Bettencourt P, Del Bono E, Spiegelman D. Clinical utility of chest auscultation in common pulmonary diseases. Am J Respir Crit Care Med 1994; 150: 1291–7.

94. Mulrow C, Lucey C, et al. Discriminating causes of dyspnea through clinical examination. J Gen Intern Med 1993; 8:383–92.

95. Epler G, Carrington C, Gaensler E. Crackles (rales) in the interstitial pulmonary diseases. Chest 1978; 73: 333–9.

96. John W, Michael R, Walter H. Medical instrumentation. Application and design. 3rd ed 1998; pp.311:312.

97. Grenier M, Gangnon K, Genest J. "Clinical Comparison of Acoustic and Electronic Stethoscopes and Design of a New Electronic Stethoscope," The American Journal of Cardiology, 1998; 81: 653-656.

98. Vannuccini L, Earis, Helistö P, Cheetham B. "Capturing and preprocessing of respiratory sounds," Eur Respir Rev, 2000; 10: 616-620.

99. Robert B, Louis N. Electronic devices and circuit theory. 7th ed. 2007; pp. 609:621.

100. James S. Physics, the instructor's edition. 3rd ed. 2007; pp. 431:444.

101. Walt J. Op amp application handbook. Analog devices. 2005; pp. 423.

102. Mark H. fundamentals of discrete Fourier transform. Sound & vibration magazine. 1978; pp. 1-2.

103. Dogan I. Advanced PIC Microcontroller projects in C, from USB to RTOS with the PIC18F series, 2008; pp 6-13.

104. Johnson N. Phagosomal p and glass fiber dissolution in cultured nasal epithelial cells and alveolar macrophages: a preliminary study. Environ Health Perspect 1994; 102: 97-103.

105. Nilsen A, Nyberg K, Camner P. Intraphagosomal pH in alveolar macrophages after phagocytosis in vivo and *in vitro* of fluoresceinlabeled yeast particles. Exp Lung Res 1988; 14: 197-207.

106. Kreyling W. Intracellular particle dissolution in alveolar macrophages. Environ Health Perspect 1992; 97: 121-6.

107. Watrous R, Grove D, Bowen D. Methods and results in characterizing electronic stethoscopes. Computers in cardiology 2002; 29: 635- 656.

108. Yashaswini B, Satyanarayana B. the design of an electronic stethoscope-review. ICCSI, march 2012.

109. Mangione S, Nieman L. "cardiac Ausculatory Skills of Internal Medicine and Family Practice Trainee" J.Am. Med. Assoc., 1997; 278: 717-722.

110. Vannuccini L, Earis J, Helistö P. "Capturing and preprocessing of respiratory sounds," Eur Respir Rev, 2000; 10: 616-620.

111. El-Segaier M. Digital Analysis of Cardiac Acoustic Signals in Children, 2007, University of Lund: Lund.

112. Liang, H., S. Lukkarinen, and I. Hartimo. Heart sound segmentation algorithm based on heart sound envelogram. In Computers in Cardiology 1997.

113. Martínez-Alajarín, J, Ruiz-Merino R. Efficient Method for Events Detection in Phonocardiographic Signals. SPIE Proceedings, 2005; 5839: 398-409.

114. Naseri, H. Homaeinezhad M. Detection and boundary identification of phonocardiogram sounds using an expert frequency-energy based metric. Ann Biomed Eng, 2013; 41: 279-92.

115. Arathy R, Gowriprabha V, Vysakh V. Pc based heart sound monitoring system. IJCA 2013; 83:1-5

116. Sovijärvi A, Malmberg L, Charbonneau G, et al. Characteristics of breath sounds and adventitious respiratory sounds. Eur Respir Rev. 2000; 10:591–596.

117. Sahgal N. Monitoring and analysis of lung sounds remotely. International Journal of COPD 2011; 6: 407 -412.

118. Mulligan K, Adler A, Gobran R. Monitoring lung diseases using electronic stethoscope arrays. Systems and computer engineering. 2009; pp 1- 4.

FFT

FFT.cpp

**********//*!

\file FFT.cpp
\brief Fast Fourier Transform routines.

This file contains a few FFT routines, including a real-FFT
routine that is almost twice as fast as a normal complex FFT,
and a power spectrum routine when you know you don't care
about phase information.

Some of this code was based on a free implementation of an FFT
by Don Cross, available on the web at:

http://www.intersrv.com/~dcross/fft.html

The basic algorithm for his code was based on Numerican Recipes
in Fortran. I optimized his code further by reducing array
accesses, caching the bit reversal table, and eliminating
float-to-double conversions, and I added the routines to
calculate a real FFT and a real power spectrum.

*//**********/
/*
Added more window functions:
* 4: Blackman
* 5: Blackman-Harris
* 6: Welch
* 7: Gaussian(a=2.5)
* 8: Gaussian(a=3.5)
* 9: Gaussian(a=4.5)
*/

```
#include <wx/intl.h>
#include <stdlib.h>
#include <stdio.h>
#include <math.h>

#include "FFT.h"

static int **gFFTBitTable = NULL;
static const int MaxFastBits = 16;
```

```
/* Declare Static functions */
static int IsPowerOfTwo(int x);
static int NumberOfBitsNeeded(int PowerOfTwo);
static int ReverseBits(int index, int NumBits);
static void InitFFT();

int IsPowerOfTwo(int x)
{
  if (x < 2)
    return false;

  if (x & (x - 1))
    return false;

  return true;
}

int NumberOfBitsNeeded(int PowerOfTwo)
{
  int i;

  if (PowerOfTwo < 2) {
    fprintf(stderr, "Error: FFT called with size %d\n", PowerOfTwo);
    exit(1);
  }

  for (i = 0;; i++)
    if (PowerOfTwo & (1 << i))
      return i;
}

int ReverseBits(int index, int NumBits)
{
  int i, rev;

  for (i = rev = 0; i < NumBits; i++) {
    rev = (rev << 1) | (index & 1);
    index >>= 1;
  }

  return rev;
}

void InitFFT()
{
  gFFTBitTable = new int *[MaxFastBits];

  int len = 2;
```

```
  for (int b = 1; b <= MaxFastBits; b++) {

    gFFTBitTable[b - 1] = new int[len];

    for (int i = 0; i < len; i++)
      gFFTBitTable[b - 1][i] = ReverseBits(i, b);

    len <<= 1;
  }
}

#ifdef EXPERIMENTAL_USE_REALFFTF
#include "RealFFTf.h"
#endif

void DeinitFFT()
{
  if (gFFTBitTable) {
    for (int b = 1; b <= MaxFastBits; b++) {
      delete[] gFFTBitTable[b-1];
    }
    delete[] gFFTBitTable;
  }
#ifdef EXPERIMENTAL_USE_REALFFTF
  // Deallocate any unused RealFFTf tables
  CleanupFFT();
#endif
}

inline int FastReverseBits(int i, int NumBits)
{
  if (NumBits <= MaxFastBits)
    return gFFTBitTable[NumBits - 1][i];
  else
    return ReverseBits(i, NumBits);
}

/*
 * Complex Fast Fourier Transform
 */

void FFT(int NumSamples,
       bool InverseTransform,
       float *RealIn, float *ImagIn, float *RealOut, float *ImagOut)
{
  int NumBits;              /* Number of bits needed to store indices */
  int i, j, k, n;
  int BlockSize, BlockEnd;
```

```
double angle_numerator = 2.0 * M_PI;
double tr, ti;              /* temp real, temp imaginary */

if (!IsPowerOfTwo(NumSamples)) {
  fprintf(stderr, "%d is not a power of two\n", NumSamples);
  exit(1);
}

if (!gFFTBitTable)
  InitFFT();

if (!InverseTransform)
  angle_numerator = -angle_numerator;

NumBits = NumberOfBitsNeeded(NumSamples);

/*
 **   Do simultaneous data copy and bit-reversal ordering into outputs...
 */

for (i = 0; i < NumSamples; i++) {
  j = FastReverseBits(i, NumBits);
  RealOut[j] = RealIn[i];
  ImagOut[j] = (ImagIn == NULL) ? 0.0 : ImagIn[i];
}

/*
 **   Do the FFT itself...
 */

BlockEnd = 1;
for (BlockSize = 2; BlockSize <= NumSamples; BlockSize <<= 1) {

  double delta_angle = angle_numerator / (double) BlockSize;

  double sm2 = sin(-2 * delta_angle);
  double sm1 = sin(-delta_angle);
  double cm2 = cos(-2 * delta_angle);
  double cm1 = cos(-delta_angle);
  double w = 2 * cm1;
  double ar0, ar1, ar2, ai0, ai1, ai2;

  for (i = 0; i < NumSamples; i += BlockSize) {
    ar2 = cm2;
    ar1 = cm1;

    ai2 = sm2;
```

```
      ai1 = sm1;

      for (j = i, n = 0; n < BlockEnd; j++, n++) {
        ar0 = w * ar1 - ar2;
        ar2 = ar1;
        ar1 = ar0;

        ai0 = w * ai1 - ai2;
        ai2 = ai1;
        ai1 = ai0;

        k = j + BlockEnd;
        tr = ar0 * RealOut[k] - ai0 * ImagOut[k];
        ti = ar0 * ImagOut[k] + ai0 * RealOut[k];

        RealOut[k] = RealOut[j] - tr;
        ImagOut[k] = ImagOut[j] - ti;

        RealOut[j] += tr;
        ImagOut[j] += ti;
      }
    }

    BlockEnd = BlockSize;
  }

  /*
    **   Need to normalize if inverse transform...
   */

  if (InverseTransform) {
    float denom = (float) NumSamples;

    for (i = 0; i < NumSamples; i++) {
      RealOut[i] /= denom;
      ImagOut[i] /= denom;
    }
  }
}

/*
 * Real Fast Fourier Transform
 *
 * This function was based on the code in Numerical Recipes in C.
 * In Num. Rec., the inner loop is based on a single 1-based array
 * of interleaved real and imaginary numbers.  Because we have two
 * separate zero-based arrays, our indices are quite different.
 * Here is the correspondence between Num. Rec. indices and our indices:
```

```
 *
 * i1  <->  real[i]
 * i2  <->  imag[i]
 * i3  <->  real[n/2-i]
 * i4  <->  imag[n/2-i]
 */

void RealFFT(int NumSamples, float *RealIn, float *RealOut, float *ImagOut)
{
#ifdef EXPERIMENTAL_USE_REALFFTF
  // Remap to RealFFTf() function
  int i;
  HFFT hFFT = GetFFT(NumSamples);
  float *pFFT = new float[NumSamples];
  // Copy the data into the processing buffer
  for(i=0; i<NumSamples; i++)
    pFFT[i] = RealIn[i];

  // Perform the FFT
  RealFFTf(pFFT, hFFT);

  // Copy the data into the real and imaginary outputs
  for(i=1;i<(NumSamples/2);i++) {
    RealOut[i]=pFFT[hFFT->BitReversed[i]  ];
    ImagOut[i]=pFFT[hFFT->BitReversed[i]+1];
  }
  // Handle the (real-only) DC and Fs/2 bins
  RealOut[0] = pFFT[0];
  RealOut[i] = pFFT[1];
  ImagOut[0] = ImagOut[i] = 0;
  // Fill in the upper half using symmetry properties
  for(i++ ; i<NumSamples; i++) {
    RealOut[i] =  RealOut[NumSamples-i];
    ImagOut[i] = -ImagOut[NumSamples-i];
  }
  delete [] pFFT;
  ReleaseFFT(hFFT);

#else

  int Half = NumSamples / 2;
  int i;

  float theta = M_PI / Half;

  float *tmpReal = new float[Half];
  float *tmpImag = new float[Half];
```

```
  for (i = 0; i < Half; i++) {
    tmpReal[i] = RealIn[2 * i];
    tmpImag[i] = RealIn[2 * i + 1];
  }

  FFT(Half, 0, tmpReal, tmpImag, RealOut, ImagOut);

  float wtemp = float (sin(0.5 * theta));

  float wpr = -2.0 * wtemp * wtemp;
  float wpi = -1.0 * float (sin(theta));
  float wr = 1.0 + wpr;
  float wi = wpi;

  int i3;

  float h1r, h1i, h2r, h2i;

  for (i = 1; i < Half / 2; i++) {

    i3 = Half - i;

    h1r = 0.5 * (RealOut[i] + RealOut[i3]);
    h1i = 0.5 * (ImagOut[i] - ImagOut[i3]);
    h2r = 0.5 * (ImagOut[i] + ImagOut[i3]);
    h2i = -0.5 * (RealOut[i] - RealOut[i3]);

    RealOut[i] = h1r + wr * h2r - wi * h2i;
    ImagOut[i] = h1i + wr * h2i + wi * h2r;
    RealOut[i3] = h1r - wr * h2r + wi * h2i;
    ImagOut[i3] = -h1i + wr * h2i + wi * h2r;

    wr = (wtemp = wr) * wpr - wi * wpi + wr;
    wi = wi * wpr + wtemp * wpi + wi;
  }

  RealOut[0] = (h1r = RealOut[0]) + ImagOut[0];
  ImagOut[0] = h1r - ImagOut[0];

  delete[]tmpReal;
  delete[]tmpImag;
#endif //EXPERIMENTAL_USE_REALFFTF
}

#ifdef EXPERIMENTAL_USE_REALFFTF
/*
 * InverseRealFFT
 *
```

```
 * This function computes the inverse of RealFFT, above.
 * The RealIn and ImagIn is assumed to be conjugate-symmetric
 * and as a result the output is purely real.
 * Only the first half of RealIn and ImagIn are used due to this
 * symmetry assumption.
 */
void InverseRealFFT(int NumSamples, float *RealIn, float *ImagIn, float *RealOut)
{
  // Remap to RealFFTf() function
  int i;
  HFFT hFFT = GetFFT(NumSamples);
  float *pFFT = new float[NumSamples];
  // Copy the data into the processing buffer
  for(i=0; i<(NumSamples/2); i++)
    pFFT[2*i  ] = RealIn[i];
  if(ImagIn == NULL) {
    for(i=0; i<(NumSamples/2); i++)
      pFFT[2*i+1] = 0;
  } else {
    for(i=0; i<(NumSamples/2); i++)
      pFFT[2*i+1] = ImagIn[i];
  }
  // Put the fs/2 component in the imaginary part of the DC bin
  pFFT[1] = RealIn[i];

  // Perform the FFT
  InverseRealFFTf(pFFT, hFFT);

  // Copy the data to the (purely real) output buffer
  ReorderToTime(hFFT, pFFT, RealOut);

  delete [] pFFT;
  ReleaseFFT(hFFT);
}
#endif // EXPERIMENTAL_USE_REALFFTF

/*
 * PowerSpectrum
 *
 * This function computes the same as RealFFT, above, but
 * adds the squares of the real and imaginary part of each
 * coefficient, extracting the power and throwing away the
 * phase.
 *
 * For speed, it does not call RealFFT, but duplicates some
 * of its code.
 */
```

```
void PowerSpectrum(int NumSamples, float *In, float *Out)
{
#ifdef EXPERIMENTAL_USE_REALFFTF
  // Remap to RealFFTf() function
  int i;
  HFFT hFFT = GetFFT(NumSamples);
  float *pFFT = new float[NumSamples];
  // Copy the data into the processing buffer
  for(i=0; i<NumSamples; i++)
    pFFT[i] = In[i];

  // Perform the FFT
  RealFFTf(pFFT, hFFT);

  // Copy the data into the real and imaginary outputs
  for(i=1;i<NumSamples/2;i++) {
    Out[i]= (pFFT[hFFT->BitReversed[i]  ]*pFFT[hFFT->BitReversed[i]  ])
      + (pFFT[hFFT->BitReversed[i]+1]*pFFT[hFFT->BitReversed[i]+1]);
  }
  // Handle the (real-only) DC and Fs/2 bins
  Out[0] = pFFT[0]*pFFT[0];
  Out[i] = pFFT[1]*pFFT[1];
  delete [] pFFT;
  ReleaseFFT(hFFT);

#else // EXPERIMENTAL_USE_REALFFTF

  int Half = NumSamples / 2;
  int i;

  float theta = M_PI / Half;

  float *tmpReal = new float[Half];
  float *tmpImag = new float[Half];
  float *RealOut = new float[Half];
  float *ImagOut = new float[Half];

  for (i = 0; i < Half; i++) {
    tmpReal[i] = In[2 * i];
    tmpImag[i] = In[2 * i + 1];
  }

  FFT(Half, 0, tmpReal, tmpImag, RealOut, ImagOut);

  float wtemp = float (sin(0.5 * theta));

  float wpr = -2.0 * wtemp * wtemp;
  float wpi = -1.0 * float (sin(theta));
```

```
  float wr = 1.0 + wpr;
  float wi = wpi;

  int i3;

  float h1r, h1i, h2r, h2i, rt, it;

  for (i = 1; i < Half / 2; i++) {

    i3 = Half - i;

    h1r = 0.5 * (RealOut[i] + RealOut[i3]);
    h1i = 0.5 * (ImagOut[i] - ImagOut[i3]);
    h2r = 0.5 * (ImagOut[i] + ImagOut[i3]);
    h2i = -0.5 * (RealOut[i] - RealOut[i3]);

    rt = h1r + wr * h2r - wi * h2i;
    it = h1i + wr * h2i + wi * h2r;

    Out[i] = rt * rt + it * it;

    rt = h1r - wr * h2r + wi * h2i;
    it = -h1i + wr * h2i + wi * h2r;

    Out[i3] = rt * rt + it * it;

    wr = (wtemp = wr) * wpr - wi * wpi + wr;
    wi = wi * wpr + wtemp * wpi + wi;
  }

  rt = (h1r = RealOut[0]) + ImagOut[0];
  it = h1r - ImagOut[0];
  Out[0] = rt * rt + it * it;

  rt = RealOut[Half / 2];
  it = ImagOut[Half / 2];
  Out[Half / 2] = rt * rt + it * it;

  delete[]tmpReal;
  delete[]tmpImag;
  delete[]RealOut;
  delete[]ImagOut;
#endif // EXPERIMENTAL_USE_REALFFTF
}

/*
 * Windowing Functions
 */
```

```
int NumWindowFuncs()
{
  return 10;
}

const wxChar *WindowFuncName(int whichFunction)
{
  switch (whichFunction) {
  default:
  case 0:
    return _("Rectangular");
  case 1:
    return wxT("Bartlett");
  case 2:
    return wxT("Hamming");
  case 3:
    return wxT("Hanning");
  case 4:
    return wxT("Blackman");
  case 5:
    return wxT("Blackman-Harris");
  case 6:
    return wxT("Welch");
  case 7:
    return wxT("Gaussian(a=2.5)");
  case 8:
    return wxT("Gaussian(a=3.5)");
  case 9:
    return wxT("Gaussian(a=4.5)");
  }
}

void WindowFunc(int whichFunction, int NumSamples, float *in)
{
  int i;
  double A;

  switch( whichFunction )
  {
  case 1:
    // Bartlett (triangular) window
    for (i = 0; i < NumSamples / 2; i++) {
      in[i] *= (i / (float) (NumSamples / 2));
      in[i + (NumSamples / 2)] *=
         (1.0 - (i / (float) (NumSamples / 2)));
    }
    break;
```

```
  case 2:
    // Hamming
    for (i = 0; i < NumSamples; i++)
      in[i] *= 0.54 - 0.46 * cos(2 * M_PI * i / (NumSamples - 1));
    break;
  case 3:
    // Hanning
    for (i = 0; i < NumSamples; i++)
      in[i] *= 0.50 - 0.50 * cos(2 * M_PI * i / (NumSamples - 1));
    break;
  case 4:
    // Blackman
    for (i = 0; i < NumSamples; i++) {
      in[i] *= 0.42 - 0.5 * cos (2 * M_PI * i / (NumSamples - 1)) + 0.08 * cos (4 * M_PI * i / (NumSamples -
1));
    }
    break;
  case 5:
    // Blackman-Harris
    for (i = 0; i < NumSamples; i++) {
      in[i] *= 0.35875 - 0.48829 * cos(2 * M_PI * i /(NumSamples-1)) + 0.14128 * cos(4 * M_PI *
i/(NumSamples-1)) - 0.01168 * cos(6 * M_PI * i/(NumSamples-1));
    }
    break;
  case 6:
    // Welch
    for (i = 0; i < NumSamples; i++) {
      in[i] *= 4*i/(float)NumSamples*(1-(i/(float)NumSamples));
    }
    break;
  case 7:
    // Gaussian (a=2.5)
    // Precalculate some values, and simplify the fmla to try and reduce overhead
    A=-2*2.5*2.5;

    for (i = 0; i < NumSamples; i++) {
      // full
      // in[i] *= exp(-0.5*(A*((i-NumSamples/2)/NumSamples/2))*(A*((i-
NumSamples/2)/NumSamples/2)));
      // reduced
      in[i] *= exp(A*(0.25 + ((i/(float)NumSamples)*(i/(float)NumSamples)) - (i/(float)NumSamples)));
    }
    break;
  case 8:
    // Gaussian (a=3.5)
    A=-2*3.5*3.5;
    for (i = 0; i < NumSamples; i++) {
      // reduced
```

```
      in[i] *= exp(A*(0.25 + ((i/(float)NumSamples)*(i/(float)NumSamples)) - (i/(float)NumSamples)));
    }
    break;
  case 9:
    // Gaussian (a=4.5)
    A=-2*4.5*4.5;

    for (i = 0; i < NumSamples; i++) {
      // reduced
      in[i] *= exp(A*(0.25 + ((i/(float)NumSamples)*(i/(float)NumSamples)) - (i/(float)NumSamples)));
    }
    break;
  default:
    fprintf(stderr,"FFT::WindowFunc - Invalid window function: %d\n",whichFunction);
  }
}
```

National Semiconductor

August 2000

LM741
Operational Amplifier

General Description

The LM741 series are general purpose operational amplifiers which feature improved performance over industry standards like the LM709. They are direct, plug-in replacements for the 709C, LM201, MC1439 and 748 in most applications.

The amplifiers offer many features which make their application nearly foolproof: overload protection on the input and output, no latch-up when the common mode range is exceeded, as well as freedom from oscillations.

The LM741C is identical to the LM741/LM741A except that the LM741C has their performance guaranteed over a 0˚C to +70˚C temperature range, instead of −55˚C to +125˚C.

Features

Connection Diagrams

Metal Can Package

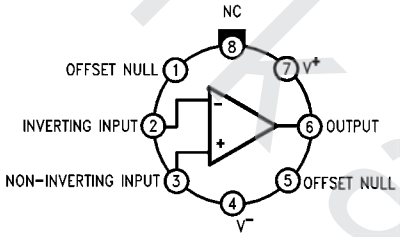

00934102

Note 1: LM741H is available per JM38510/10101

Order Number LM741H, LM741H/883 (Note 1)**, LM741AH/883 or LM741CH**
See NS Package Number H08C

Dual-In-Line or S.O. Package

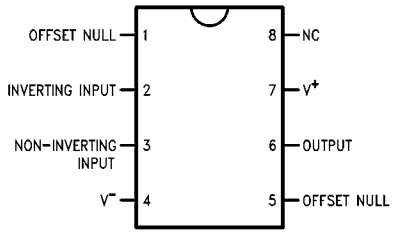

00934103

Order Number LM741J, LM741J/883, LM741CN
See NS Package Number J08A, M08A or N08E

Ceramic Flatpak

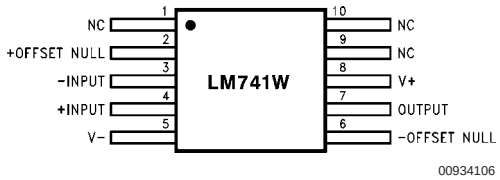

00934106

Order Number LM741W/883
See NS Package Number W10A

Typical Application

Offset Nulling Circuit

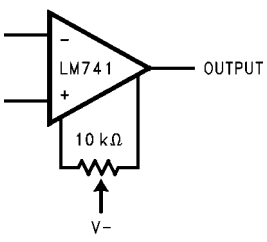

00934107

Absolute Maximum Ratings (Note 2)

If Military/Aerospace specified devices are required, please contact the National Semiconductor Sales Office/ Distributors for availability and specifications.

(Note 7)

	LM741A	LM741	LM741C
Supply Voltage	±22V	±22V	±18V
Power Dissipation (Note 3)	500 mW	500 mW	500 mW
Differential Input Voltage	±30V	±30V	±30V
Input Voltage (Note 4)	±15V	±15V	±15V
Output Short Circuit Duration	Continuous	Continuous	Continuous
Operating Temperature Range	−55˚C to +125˚C	−55˚C to +125˚C	0˚C to +70˚C
Storage Temperature Range	−65˚C to +150˚C	−65˚C to +150˚C	−65˚C to +150˚C
Junction Temperature	150˚C	150˚C	100˚C
Soldering Information			
N-Package (10 seconds)	260˚C	260˚C	260˚C
J- or H-Package (10 seconds)	300˚C	300˚C	300˚C
M-Package			
Vapor Phase (60 seconds)	215˚C	215˚C	215˚C
Infrared (15 seconds)	215˚C	215˚C	215˚C
See AN-450 "Surface Mounting Methods and Their Effect on Product Reliability" for other methods of soldering surface mount devices.			
ESD Tolerance (Note 8)	400V	400V	400V

Electrical Characteristics (Note 5)

Parameter	Conditions	LM741A			LM741			LM741C			Units
		Min	Typ	Max	Min	Typ	Max	Min	Typ	Max	
Input Offset Voltage	T_A = 25˚C										
	$R_S \le 10\ k\Omega$					1.0	5.0		2.0	6.0	mV
	$R_S \le 50\Omega$		0.8	3.0							mV
	$T_{AMIN} \le T_A \le T_{AMAX}$										
	$R_S \le 50\Omega$			4.0							mV
	$R_S \le 10\ k\Omega$						6.0			7.5	mV
Average Input Offset Voltage Drift				15							µV/˚C
Input Offset Voltage Adjustment Range	T_A = 25˚C, V_S = ±20V	±10				±15			±15		mV
Input Offset Current	T_A = 25˚C		3.0	30		20	200		20	200	nA
	$T_{AMIN} \le T_A \le T_{AMAX}$			70		85	500			300	nA
Average Input Offset Current Drift				0.5							nA/˚C
Input Bias Current	T_A = 25˚C		30	80		80	500		80	500	nA
	$T_{AMIN} \le T_A \le T_{AMAX}$			0.210			1.5			0.8	µA
Input Resistance	T_A = 25˚C, V_S = ±20V	1.0	6.0		0.3	2.0		0.3	2.0		MΩ
	$T_{AMIN} \le T_A \le T_{AMAX}$, V_S = ±20V	0.5									MΩ
Input Voltage Range	T_A = 25˚C							±12	±13		V
	$T_{AMIN} \le T_A \le T_{AMAX}$				±12	±13					V

Electrical Characteristics (Note 5) (Continued)

Parameter	Conditions	LM741A			LM741			LM741C			Units
		Min	Typ	Max	Min	Typ	Max	Min	Typ	Max	
Large Signal Voltage Gain	$T_A = 25^\circ C$, $R_L \geq 2\ k\Omega$										
	$V_S = \pm 20V$, $V_O = \pm 15V$	50									V/mV
	$V_S = \pm 15V$, $V_O = \pm 10V$				50	200		20	200		V/mV
	$T_{AMIN} \leq T_A \leq T_{AMAX}$,										
	$R_L \geq 2\ k\Omega$,										
	$V_S = \pm 20V$, $V_O = \pm 15V$	32									V/mV
	$V_S = \pm 15V$, $V_O = \pm 10V$				25			15			V/mV
	$V_S = \pm 5V$, $V_O = \pm 2V$	10									V/mV
Output Voltage Swing	$V_S = \pm 20V$										
	$R_L \geq 10\ k\Omega$	±16									V
	$R_L \geq 2\ k\Omega$	±15									V
	$V_S = \pm 15V$										
	$R_L \geq 10\ k\Omega$				±12	±14		±12	±14		V
	$R_L \geq 2\ k\Omega$				±10	±13		±10	±13		V
Output Short Circuit	$T_A = 25^\circ C$	10	25	35		25			25		mA
Current	$T_{AMIN} \leq T_A \leq T_{AMAX}$	10		40							mA
Common-Mode	$T_{AMIN} \leq T_A \leq T_{AMAX}$										
Rejection Ratio	$R_S \leq 10\ k\Omega$, $V_{CM} = \pm 12V$				70	90		70	90		dB
	$R_S \leq 50\Omega$, $V_{CM} = \pm 12V$	80	95								dB
Supply Voltage Rejection	$T_{AMIN} \leq T_A \leq T_{AMAX}$,										
Ratio	$V_S = \pm 20V$ to $V_S = \pm 5V$										
	$R_S \leq 50\Omega$	86	96								dB
	$R_S \leq 10\ k\Omega$				77	96		77	96		dB
Transient Response	$T_A = 25^\circ C$, Unity Gain										
Rise Time			0.25	0.8		0.3			0.3		µs
Overshoot			6.0	20		5			5		%
Bandwidth (Note 6)	$T_A = 25^\circ C$	0.437	1.5								MHz
Slew Rate	$T_A = 25^\circ C$, Unity Gain	0.3	0.7			0.5			0.5		V/µs
Supply Current	$T_A = 25^\circ C$					1.7	2.8		1.7	2.8	mA
Power Consumption	$T_A = 25^\circ C$										
	$V_S = \pm 20V$		80	150							mW
	$V_S = \pm 15V$					50	85		50	85	mW
LM741A	$V_S = \pm 20V$										
	$T_A = T_{AMIN}$			165							mW
	$T_A = T_{AMAX}$			135							mW
LM741	$V_S = \pm 15V$										
	$T_A = T_{AMIN}$					60	100				mW
	$T_A = T_{AMAX}$					45	75				mW

Note 2: "Absolute Maximum Ratings" indicate limits beyond which damage to the device may occur. Operating Ratings indicate conditions for which the device is functional, but do not guarantee specific performance limits.

Electrical Characteristics (Note 5) (Continued)

Note 3: For operation at elevated temperatures, these devices must be derated based on thermal resistance, and T_j max. (listed under "Absolute Maximum Ratings"). $T_j = T_A + (\theta_{jA} P_D)$.

Thermal Resistance	Cerdip (J)	DIP (N)	HO8 (H)	SO-8 (M)
θ_{jA} (Junction to Ambient)	100˚C/W	100˚C/W	170˚C/W	195˚C/W
θ_{jC} (Junction to Case)	N/A	N/A	25˚C/W	N/A

Note 4: For supply voltages less than ±15V, the absolute maximum input voltage is equal to the supply voltage.

Note 5: Unless otherwise specified, these specifications apply for V_S = ±15V, −55˚C ≤ T_A ≤ +125˚C (LM741/LM741A). For the LM741C/LM741E, these specifications are limited to 0˚C ≤ T_A ≤ +70˚C.

Note 6: Calculated value from: BW (MHz) = 0.35/Rise Time(µs).

Note 7: For military specifications see RETS741X for LM741 and RETS741AX for LM741A.

Note 8: Human body model, 1.5 kΩ in series with 100 pF.

Schematic Diagram

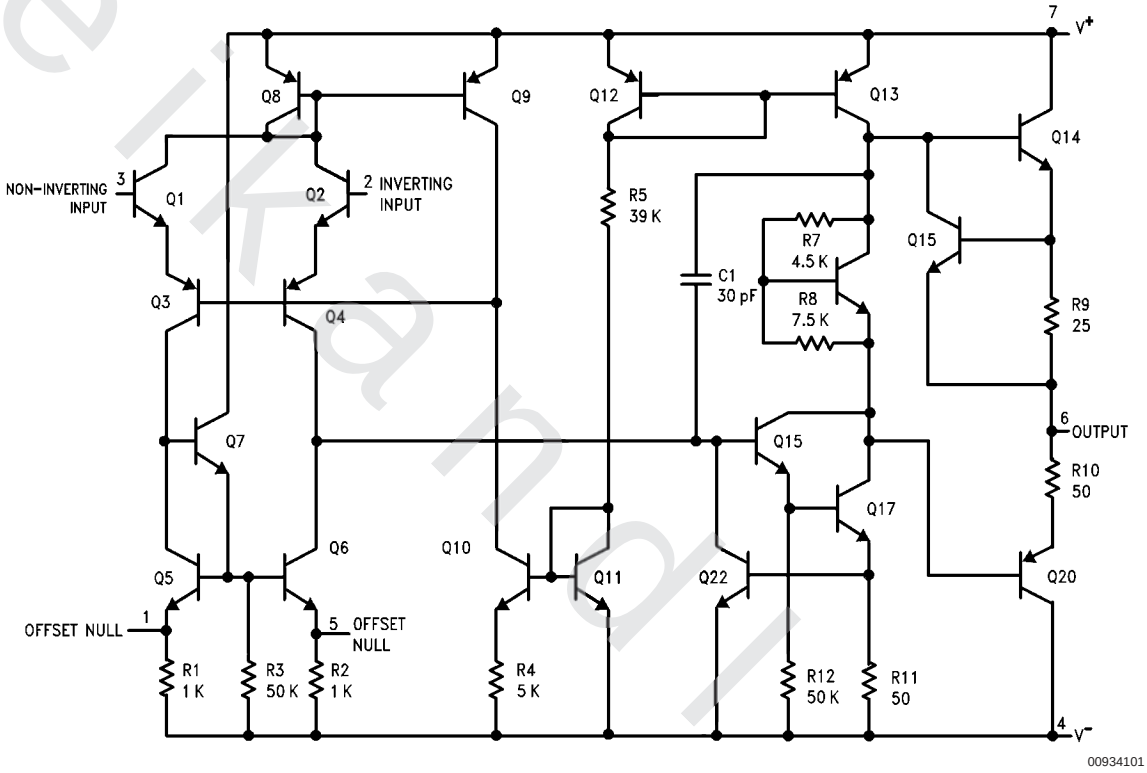

Physical Dimensions inches (millimeters)
unless otherwise noted

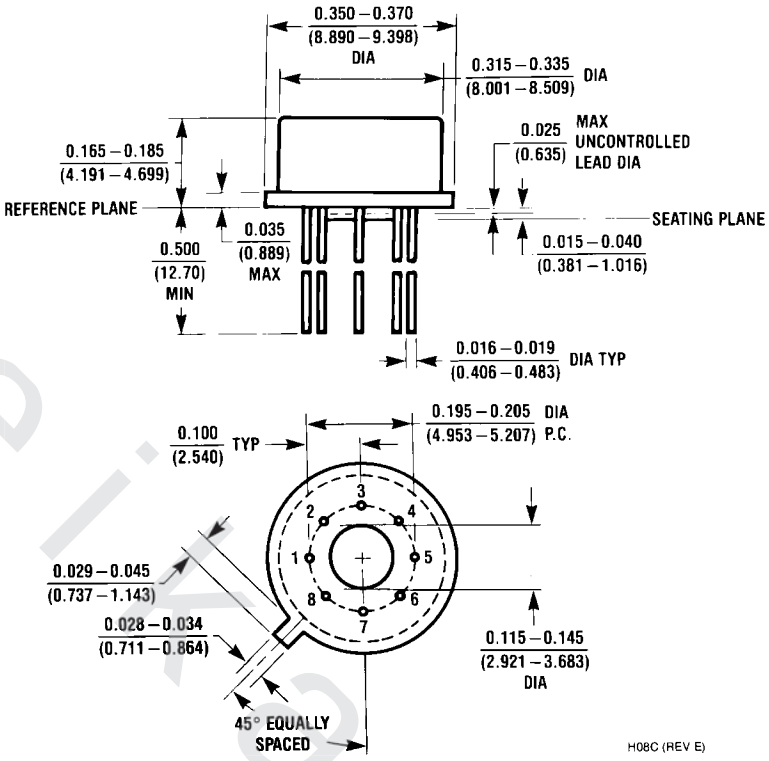

Metal Can Package (H)
Order Number LM741H, LM741H/883, LM741AH/883, LM741AH-MIL or LM741CH
NS Package Number H08C

Physical Dimensions inches (millimeters) unless otherwise noted (Continued)

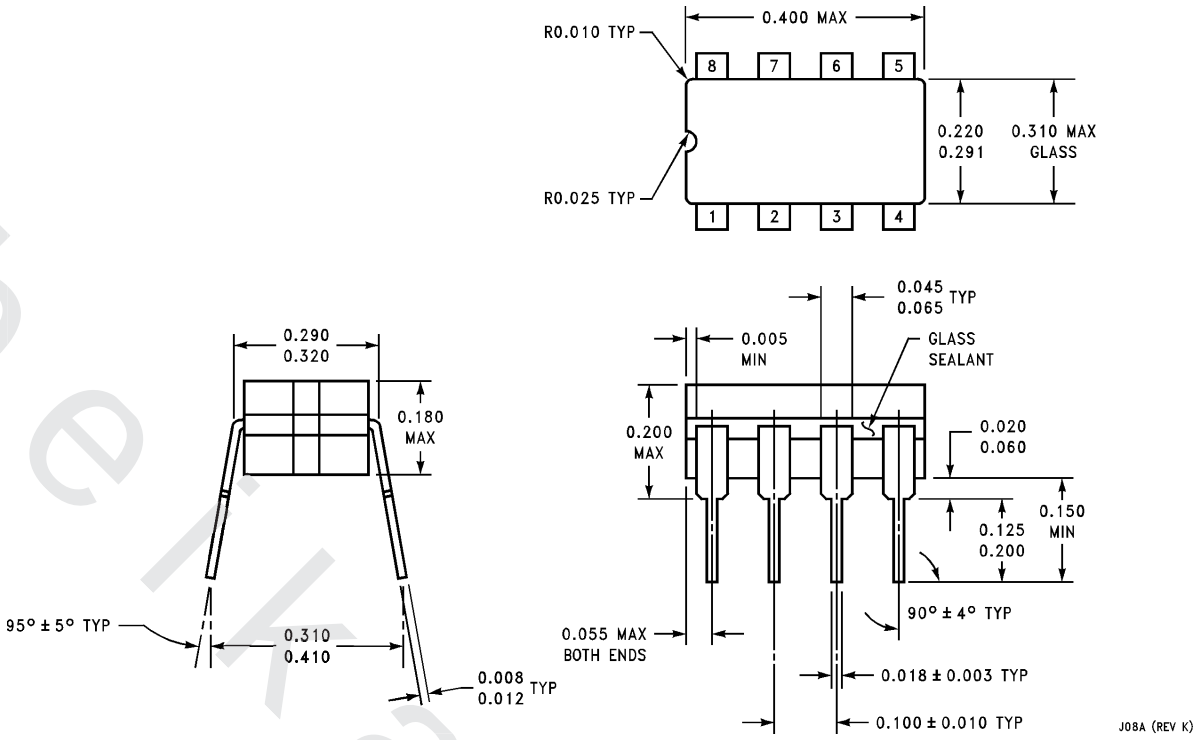

Ceramic Dual-In-Line Package (J)
Order Number LM741J/883
NS Package Number J08A

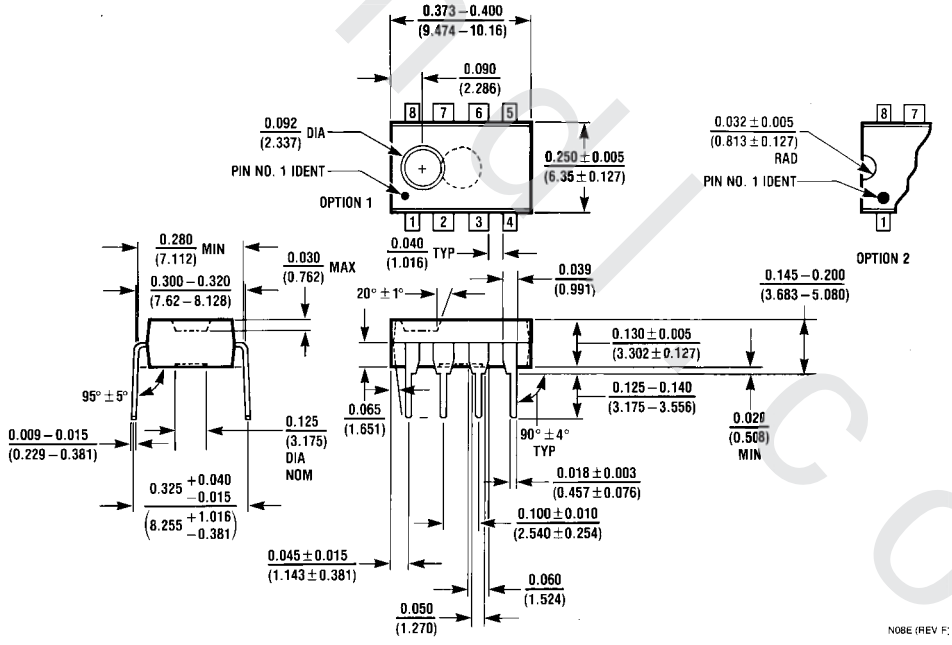

Dual-In-Line Package (N)
Order Number LM741CN
NS Package Number N08E

Physical Dimensions inches (millimeters) unless otherwise noted (Continued)

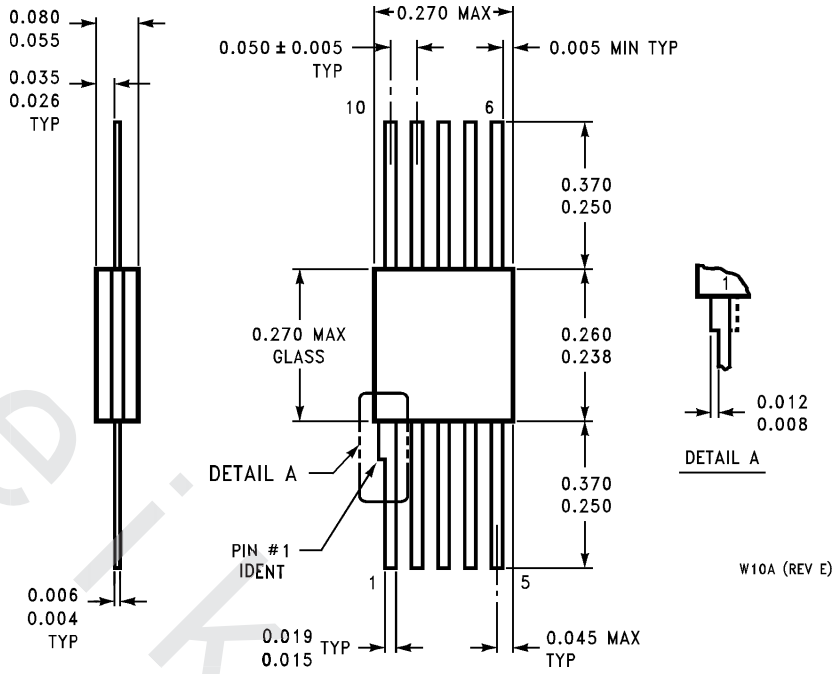

10-Lead Ceramic Flatpak (W)
Order Number LM741W/883, LM741WG-MPR or LM741WG/883
NS Package Number W10A

National Semiconductor
Americas Customer
Support Center
Email: new.feedback@nsc.com
Tel: 1-800-272-9959

www.national.com

National Semiconductor
Europe Customer Support Center
Fax: +49 (0) 180-530 85 86
Email: europe.support@nsc.com
Deutsch Tel: +49 (0) 69 9508 6208
English Tel: +44 (0) 870 24 0 2171
Français Tel: +33 (0) 1 41 91 8790

National Semiconductor
Asia Pacific Customer
Support Center
Email: ap.support@nsc.com

National Semiconductor
Japan Customer Support Center
Fax: 81-3-5639-7507
Email: jpn.feedback@nsc.com
Tel: 81-3-5639-7560

PART NUMBER: CMA-4544PF-W **DESCRIPTION:** electret condenser microphone

SPECIFICATIONS

directivity	omnidirectional	
sensitivity (S)	-44 ±2 dB	f = 1KHz, 1Pa 0dB = 1V/Pa
sensitivity reduction (ΔS-Vs)	-3 dB	f = 1KHz, 1Pa Vs = 3.0 ~ 2.0 V dc
operating voltage	3 V dc (standard), 10 V dc (max.)	
output impedance (Zout)	2.2 KΩ	f = 1KHz, 1Pa
operating frequency (f)	20 ~ 20,000 Hz	
current consumption (IDSS)	0.5 mA max.	Vs = 3.0 V dc RL = 2.2KΩ
signal to noise ratio (S/N)	60 dBA	f = 1KHz, 1Pa A-weighted
operating temperature	-20 ~ +70° C	
storage temperature	-20 ~ +70° C	
dimensions	ø9.7 x 4.5 mm	
weight	0.80 g max.	
material	Al	
terminal	pin type (hand soldering only)	
RoHS	yes	

note: We use the "Pascal (Pa)" indication of sensitivity as per the recomendation of I.E.C. (International Electrotechnical Commission). The sensitivity of "Pa" will increase 20dB compared to the "ubar" indication. Example: -60dB (0dB = 1V/ubar) = -40dB (1V/Pa)

APPEARANCE DRAWING

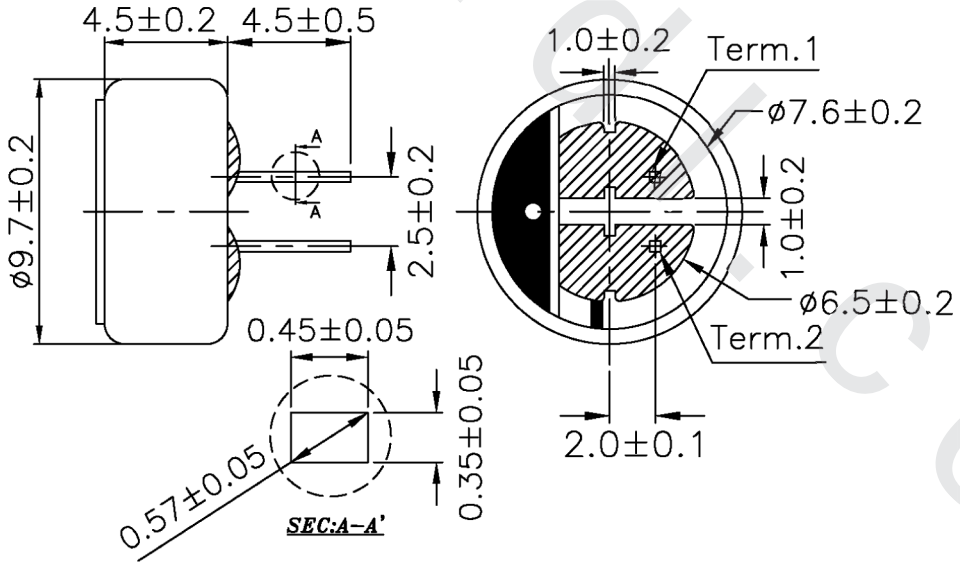

PART NUMBER: CMA-4544PF-W **DESCRIPTION:** electret condenser microphone

MEASUREMENT CIRCUIT

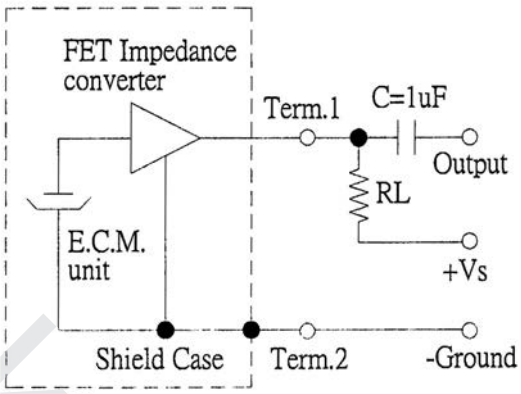

Schematic Diagram **RL=2.2KΩ**

FREQUENCY RESPONSE CURVE

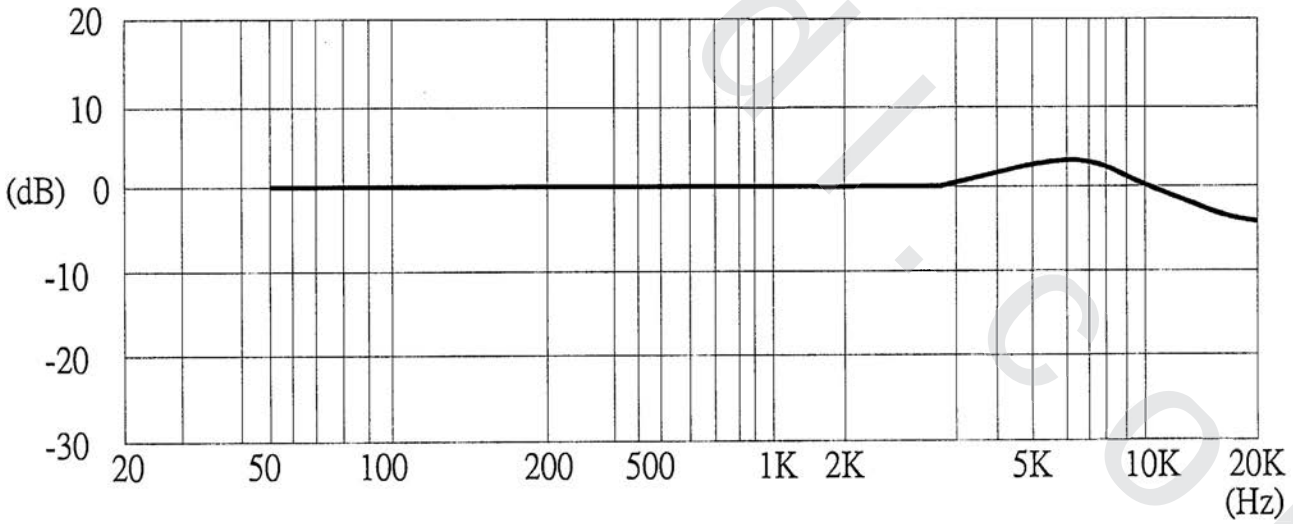

PART NUMBER: CMA-4544PF-W **DESCRIPTION:** electret condenser microphone

MECHANICAL CHARACTERISTICS

item	test condition	evaluation standard
soldering heat resistance	Lead terminals are immersed in solder bath of 270 ±5°C for 2 ±0.5 seconds.	No interference in operation.
PCB wire pull strength	The pull force will be applied to double lead wire: Horizontal 4.9N (0.5kg) for 30 seconds	No damage or cutting off.
vibration	The part will be measured after applying a vibration amplitude of 1.5 mm with 10 to 55 Hz band of vibration frequency to each of the 3 perpendicular directions for 2 hours.	After any tests, the sensitivity should be within ±3dB compared to the initial measurement.
drop test	The part will be dropped from a height of 1 m onto a 20 mm thick wooden board 3 times in 3 axes (X, Y, Z) for a total of 9 drops.	

ENVIRONMENT TEST

item	test condition	evaluation standard
high temp. test	After being placed in a chamber at +70°C for 72 hours.	The part will be measured after being placed at +25°C for 6 hours. After any tests, the sensitivity should be within ±3dB compared to the initial measurement.
low temp. test	After being placed in a chamber at -20°C for 72 hours.	
humidity test	After being placed in a chamber at +40°C and 90±5% relative humidity for 240 hours.	
temp. cycle test	The part shall be subjected to 10 cycles. One cycle will consist of: 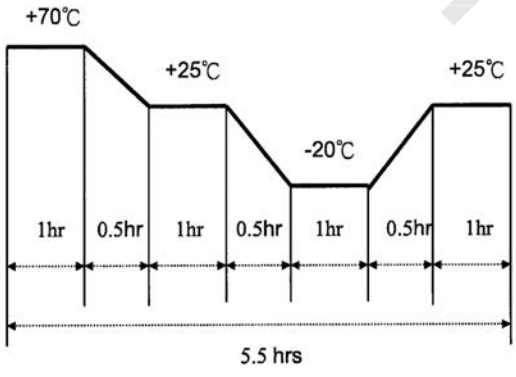 	

TEST CONDITIONS

standard test condition	a) temperature: +5 ~ +35°C	b) humidity: 45 - 85%	c) pressure: 860-1060 mbar
judgement test condition	a) temperature: +25 ±2°C	b) humidity: 60 - 70%	c) pressure: 860-1060 mbar

PART NUMBER: CMA-4544PF-W **DESCRIPTION:** electret condenser microphone

PACKAGING

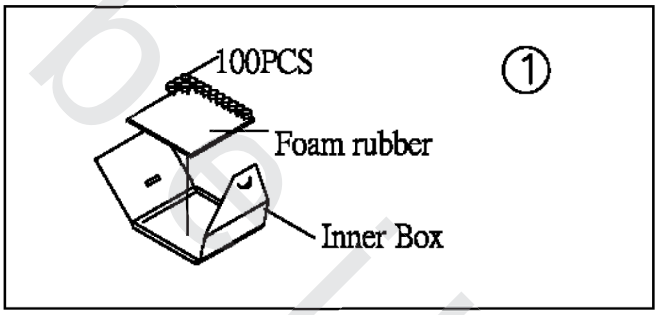

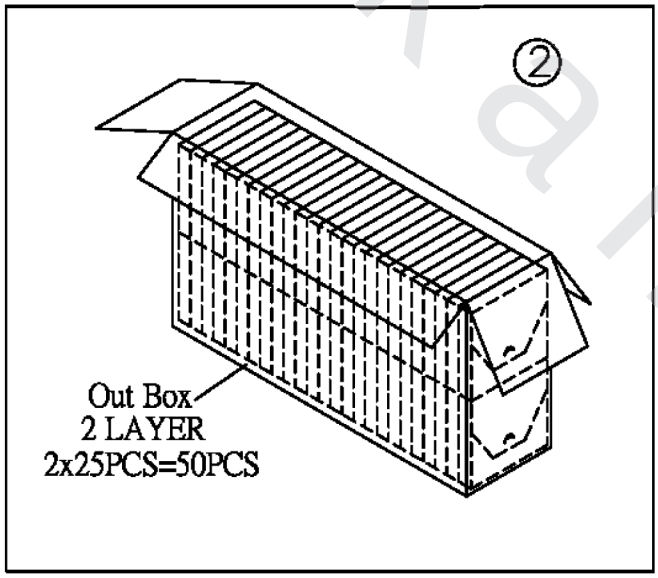

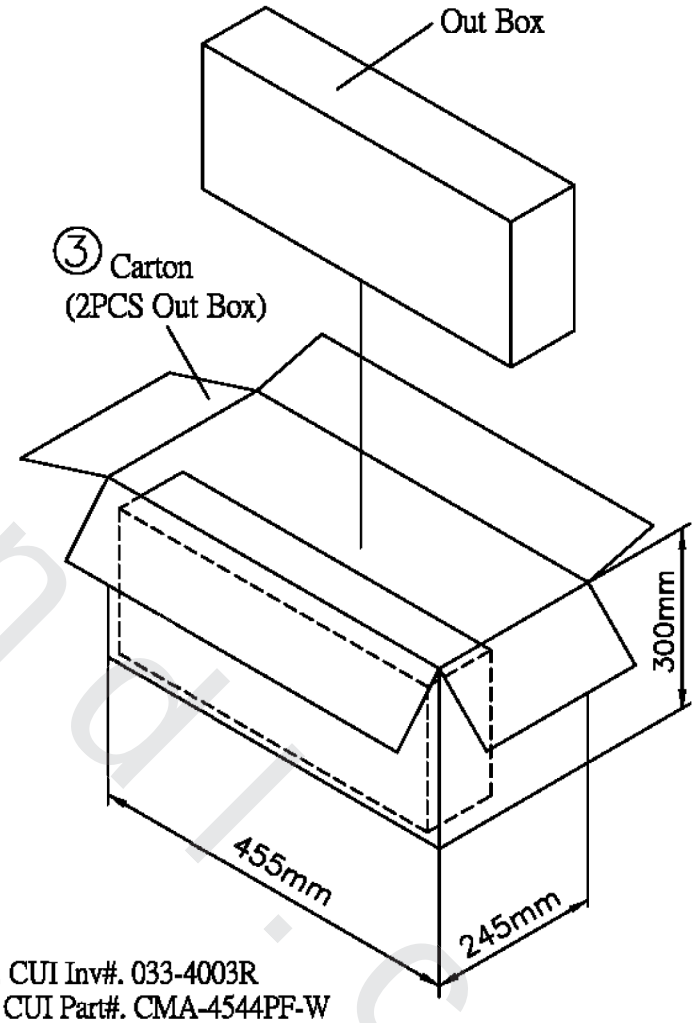

1. CUI Inv#. 033-4003R
   CUI Part#. CMA-4544PF-W
2. RoHS Compliant

Inner Box	100mmx100mmx15mm	100PCSx1=100PCS
Out Box	435mmx120mmx280mm	100PCSx50=5,000PCS
Carton Box	455mmx245mmx300mm	5,000PCSx2=10,000PCS

الملخص العربى

تبقى سماعة الطبيب محور أدوات التشخيص بالنسبة للأطباء لأداء امتحانات القلب لمرضاهم. يمكن تشخيص العديد من التشوهات القلبية والرئوية مع استخدام سماعة الطبيب. التسمع هو واحد من الاختبارات التشخيصية الأكثر فعالية من حيث التكلفة للمرضى الذين يعانون من تشوهات قلبية ورئوية.

صممت السماعات الرقمية للتغلب على عيوب السماعات الصوتية. سماعة الطبيب الرقمية تضخم الأصوات إلكترونيا . يستخدم سماعة الموجات الصوتية الرقمية، والتي يتم تحويلها من التناظرية إلى إشارات كهربائية يتم تضخيمها وتوفير الكثير من لودر وأوضح الصوت. وهذا يجعل تحديد المشاكل بشكل أسرع وأسهل، وأنه يسمح اختار تسجيل وتشغيل الأصوات تصل، مما يجعلها مفيدة للمراجع أو في التدريس للطلاب.

في العمل الحالي، تم تصميم نظام سماعة الطبيب الرقمية والتي شيدت للتغلب على القيود المفروضة على السماعات التقليدية. وهو يتألف من دائرة مولد إشارة لتوليد إشارة الصوت مع تردد والموجي المناسب للنموذج التي شيدت من قبل المتكلم مصغرة. مكثف ميكروفون electrets يتلقى إشارة الصوت وتحولها إلى إشارة كهربائية. إشارة ثم تم تضخيمها وتصفيتها مع زيادة مناسبة والتي تنتقل عن طريق كابل كهربائي لبطاقة الصوت من جهاز كمبيوتر شخصي (PC) لمزيد من الرصد والتحليل للإشارة الصوت الناتج.

أظهرت نتائج النموذج محاكاة ما يلي:

- السعة من الصوت الناتج إشارة زيادات مع زيادة من الحلول (المياه، وكلوريد الصوديوم، الجلوكوز)، وكمية الجل.
- وتوهين الصوت ومعامل التوهين يتناقص مع زيادة كمية من الحلول.

وقد تم تطوير نظام رقمي مجموعة سماعة الطبيب لرصد وتشخيص أمراض الرئة الانسدادي التي ترتبط مع تراكم السوائل في الرئة والأمراض القلبية الوعائية التي ترتبط مع نفخة القلب مثل نفخة الانقباضي والانبساطي من النقاط التسمع مختلفة.

وأظهرت نتائج تحليل سليم القلب ما يلي:

- وكانت أطياف التردد لجميع الأصوات القلب العادية وغير العادية ٦٤ هرتز.
- كان اتساع صوت القلب الطبيعي عند نقطة التسمع قمة -١٧ ديسيبل، بينما في نقاط التسمع الأبهر والرئوي كانت -١٠ ديسيبل.
- واتساع القلب غير طبيعية الأصوات كانت S3 S4 وعند نقطة التسمع قمة
- كان اتساع الانقسام S1 عند نقطة التسمع قمة -٢٢ ديسيبل، بينما كان اتساع الانقسام S2 عند نقطة التسمع الرئوي -١٦ ديسيبل.
- وكانت السعة في وقت مبكر، منتصف، في وقت متأخر وهولو الانقباضي نفخة عند نقطة التسمع قمة في نطاق -٢٤ ديسيبل إلى -٢٢ ديسيبل.

وأظهرت نتائج تحليل سليم الرئة ما يلي:

- كان اتساع كل الأصوات الرئة العادية وغير العادية في حدود -٥٠ إلى -٣٠ ديسيبل ديسيبل.
- كان الطيف الترددي من الصوت العادي الرئة الحويصلي ١٢٠ هرتز.
- الطيف تردد الخشنة الخشخشة كان الصوت ٣٣٠ هرتز.
- كان الطيف الترددي للصوت صرير الشهيق ٢٧٥ هرتز.
- كان الطيف الترددي للصوت الاحتكاك الجنبي ٥٨ هرتز.
- كان الطيف الترددي من الصفير الصوت ١٩٨ هرتز.

جامعة الإسكندرية
معهد البحوث الطبية
قسم الفيزياء الحيوية الطبية

تصميم وبناء مجموعة سماعات طبية إلكترونيه لتشخيص أمراض القلب والرئه

رسالة مقدمة

بقسم الفيزياء الحيوية الطبية ـ معهد البحوث الطبية – جامعة الإسكندرية

ضمن متطلبات درجة

الدكتوراه

فى

الفيزياء الحيوية الطبية

من

محمد سيد منصور محمد

بكالوريوس العلوم الطبية التطبيقية، جامعة ٦ أكتوبر، ٢٠٠٣
ماجستير الفيزياء الحيوية الطبية، معهد البحوث الطبية، جامعة الإسكندرية، ٢٠١١

٢٠١٤

جامعة الإسكندرية
معهد البحوث الطبية
قسم الفيزياء الحيوية الطبية

تصميم وبناء مجموعة سماعات طبية إلكترونيه لتشخيص أمراض القلب والرئه

رسالة مقدمة من

محمد سيد منصور محمد

للحصول على درجة

الدكتوراه فى الفيزياء الحيوية الطبية

لجنة المناقشة والحكم على الرسالة	**موافقون**
أ.د/ إسماعيل إبراهيم حجازى أستاذ الكيمياء الحيوية كلية الطب جامعة الأزهر بنين	----------
ا.د/ محمد كمال الدين نصره أستاذ الفيزياء الحيوية الطبية معهد البحوث الطبية جامعة الإسكندرية	----------
أ.د/ مصطفى مصطفى محمد أستاذ الفيزياء الحيوية الطبية كلية العلوم الطبية جامعة فاروس	----------
أ.د/ سهير الخولى أستاذ الفيزياء الحيوية الطبية معهد البحوث الطبية جامعة الإسكندرية	----------

التاريخ / /

المشرفون **موافقون**

الدكتور / نيفان محمود فكرى .....

أستاذ بقسم الطبيعة الحيوية الطبية

معهد البحوث الطبية

جامعة الإسكندرية

الدكتور /مصطفى مصطفى محمد .....

أستاذ الطبيعة الحيوية الطبية

بكلية العلوم الطبية التطبيقية

جامعة فاروس

الدكتور / سهير الخولى .....

أستاذ بقسم الطبيعة الحيوية الطبية

معهد البحوث الطبية

جامعة الإسكندرية

الدكتور/ محمد أحمد بندق .....

مدرس الهندسة الحيوية الطبية

بكلية العلوم الطبية التطبيقية

جامعة ٦ أكتوبر